

REVIEW

Thermal Stability and Microstructure of Bi-Sr-Ca-Cu-O Glasses

Ryuji SATO*, Takayuki KOMATSU*
and Kazumasa MATUSITA*

Received May 31, 1994

This paper reviews glass formation, thermal stability, some physical properties and structure of glasses based on the Bi-Sr-Ca-Cu-O (Bi-based) system. Especially, the effect of copper valence state on the thermal stability and microstructure of the $\text{Bi}_2\text{Sr}_2\text{CaCu}_2\text{O}_x$ glass has been clarified. The $\text{Cu}^+/\Sigma\text{Cu}$ ratio in Bi-based glasses is largely changed from 0.01 to 0.98 by adding glucose during melting or by annealing of powdered glasses in oxygen at near the glass transition temperature. The thermal stability of the glasses with high Cu^+ contents is extremely high compared with that of the glasses with low Cu^+ contents. The viscosity and density of glasses decrease steeply with increasing $\text{Cu}^+/\Sigma\text{Cu}$ ratio, implying that the structure of Bi-based glasses becomes loose with increasing Cu^+ content. The phase separation is observed in the glasses with high Cu^+ contents, but no phase separation occurs in the glasses with high Cu^{2+} contents. The correlation between the phase separation and crystallization behaviors has been discussed.

KEY WORDS: Bi-Sr-Ca-Cu-O Glasses/ Thermal Stability/ Superconducting Glass-Ceramics/ Phase separation/ $\text{Cu}^+/\Sigma\text{Cu}$

1. INTRODUCTION

Many compositions in the Bi-Sr-Ca-Cu-O system (Bi-based system) are glass-forming through the quenching of melts, and glasses are converted into high-Tc superconductors after proper annealing.¹⁻⁴⁾ This preparation technique, i.e., melt-quenching method or glass-ceramic route, is very attractive for the fabrication of superconductors with desired forms such as fibers. Many studies on superconducting properties of Bi-based glass-ceramics have been made so far. In order to fabricate superconducting glass-ceramics with more excellent properties, an in-depth understanding of the crystallization mechanism of Bi-based glasses will be necessary. It should be pointed out that a large amount (70~80%) of copper ions in the Bi-based glasses prepared by a conventional melt-quenching method exists as monovalent Cu^+ ions.⁵⁾ On the other hand, it is well known that the average copper valences in the Bi-based superconducting phases are over 2.0. It is, therefore, very important to clarify the effect of copper valence state in Bi-based glasses on crystallization behaviors.⁶⁾

Since Bi-based glasses are newcomers in the field of glass science and technology, the structure and properties of glasses themselves are also of particular interest. Recently, the effect of copper valence state on thermal stability and some properties such as viscosity and density in

* 佐藤隆士, 小松高行, 松下和正 : Department of Chemistry, Nagaoka University of Technology, Nagaoka 940-21, Japan.

Bi-based glasses has been clarified.^{5,7)} The data on the structure of Bi-based glasses seem to be insufficient at this moment. But, very recently, phase separation behaviors in Bi-based glasses have been reported.⁸⁻¹⁰⁾ In this paper, we review glass formation, thermal stability, some physical properties and structure of Bi-based glasses. Especially, we focus our attention on the effects of copper valence state on the thermal stability and microstructure of the $\text{Bi}_2\text{Sr}_2\text{CaCu}_2\text{O}_x$ glass, which also will shed some important light on the fabrication of high-performance high- T_c superconducting glass-ceramics.

2. GLASS FORMATION REGION

The glass-forming region in the Bi-Sr-Ca-Cu-O system has been reported by several groups.¹¹⁻¹⁶⁾ The glass forming-region in the $x\text{BiO}_{3/2}-y\text{SrO}-z\text{CaO}-2\text{CuO}$ system ($x=0.5\sim 3$, $y=0.5\sim 2$ and $z=0.3\sim 2$) is shown in Fig. 1.¹¹⁾ It can be seen that the $\text{BiO}_{3/2}$ -SrO-CaO-CuO system has a strong tendency to form a glass and that the addition of Bi_2O_3 is particularly effective in facilitating glass formation. The ratio of SrO and CaO is also important. Miyaji *et al.*¹²⁾ examined the glass forming regions of Bi_2O_3 -CaO-CuO and Bi_2O_3 -SrO-CuO by using a conventional melt-quenching method. They reported that glasses are more easily formed with lower Bi_2O_3 compositions in the Bi_2O_3 -SrO-CuO system than in the Bi_2O_3 -CaO-CuO system and that the structure of SrO containing glasses is considerably different from that of CaO containing glasses. Tohge *et al.*¹³⁾ also examined the glass forming region in the pseudoternary system $\text{BiO}_{3/2}$ -(SrO,Ca)_{1/2}-CuO, $\text{Ca}/\text{SrO}=1$, by using a twin-roller rapid quenching method. They reported that the amorphous samples were obtained in a relatively wide region. Since monovalent copper ions coexist with divalent ones in the Bi-based glasses, the $\text{Cu}^+/\Sigma\text{Cu}$ ratio should be specially considered for the investigation of the glass forming region. However, there

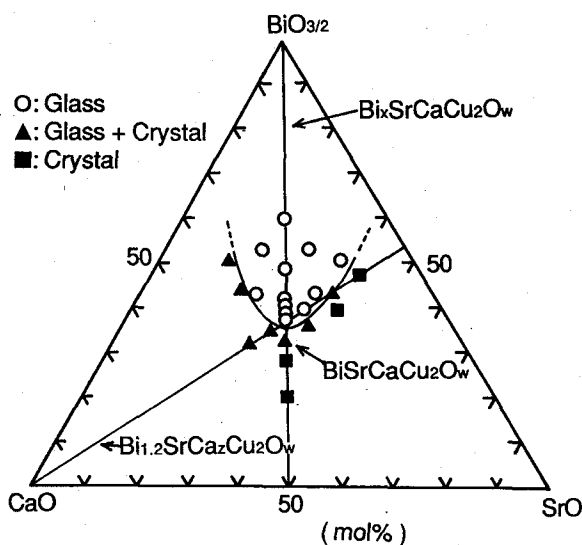


Fig. 1. The glass-forming region of the $x\text{BiO}_{3/2}-y\text{SrO}-z\text{CaO}-2\text{CuO}$ system ($x=0.5\sim 3.0$, $y=0.5\sim 2.0$, $z=0.3\sim 2.0$). The coordinates in the figure for the glass-forming region are the mol percentages of each oxide among $\text{BiO}_{3/2}$, SrO and CaO.¹¹⁾

has been no report on the effect of $\text{Cu}^+/\Sigma\text{Cu}$ ratio on the glass forming region in the Bi-based glasses.

3. THERMAL PROPERTY IN $\text{Bi}_2\text{Sr}_2\text{CaCu}_2\text{O}_x$ GLASS

The glass formation of the sample with the composition of the low- T_c phase $\text{Bi}_2\text{Sr}_2\text{CaCu}_2\text{O}_x$ has been reported by several research groups.¹⁷⁻²³⁾ For example, Yoshimura *et al.*¹⁸⁾ prepared 20 μm thick $\text{Bi}_2\text{Sr}_2\text{CaCu}_2\text{O}_x$ amorphous films by using twin-roller rapid quenching. Zheng and Mackenzie¹⁹⁾ prepared 1 mm thick $\text{Bi}_4\text{Sr}_3\text{Ca}_3\text{Cu}_4\text{O}_x$ glasses by using a conventional melt-quenching method. A differential thermal analysis (DTA) curve for the $\text{Bi}_2\text{Sr}_2\text{CaCu}_2\text{O}_x$ glass prepared by using a conventional melt-quenching method is shown in Fig. 2.²³⁾ This glass was melted using a Pt crucible. The values of glass transition, T_g , and crystallization temperatures, T_x , are 435°C and 486°C respectively.

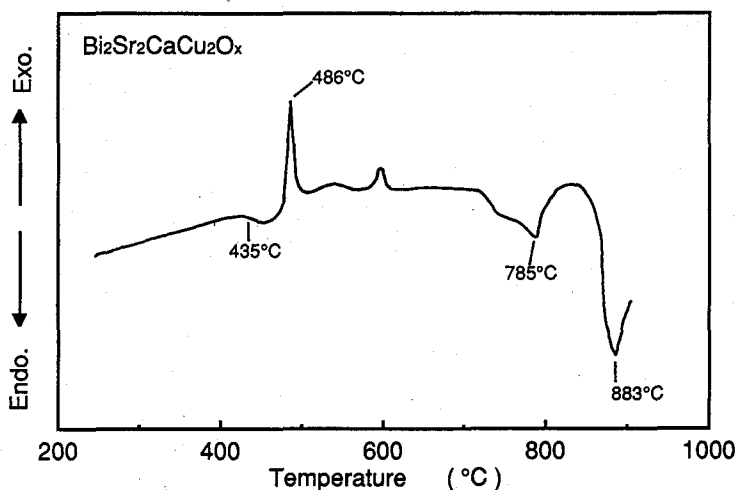


Fig. 2. DTA curve for the melt-quenched sample of $\text{Bi}_2\text{Sr}_2\text{CaCu}_2\text{O}_x$.²³⁾ Heating rate was 10 K/min.

Recently, Sato *et al.*⁵⁾ succeeded in preparing the $\text{Bi}_2\text{Sr}_2\text{CaCu}_2\text{O}_x$ glasses with various $\text{Cu}^+/\Sigma\text{Cu}$ ratios ranging from about 0.8 to 0.98 by adding glucose during glass melting and examined the effect of $\text{Cu}^+/\Sigma\text{Cu}$ ratio on the thermal stability. In their experiment, the glasses were prepared as follows; commercial powders of high-purity Bi_2O_3 , SrCO_3 , CaCO_3 and CuO were mixed and calcined at 820°C for 10 h in air. Glucose was added to calcined powders and mixed in methanol. The glucose addition was 0~2.5 wt% of batch weight. The mixture was melted in an alumina crucible at 1,300°C for 10 min in an electric furnace. The melts were poured onto an iron plate and pressed quickly to a thickness of 1.5 mm. Figure 3 shows the fractions of Cu^+ in the glass analyzed by a cerate titration method. The estimated values from thermogravimetry (TG) curves are also shown. It can be seen that the $\text{Cu}^+/\Sigma\text{Cu}$ ratio increases with increasing glucose content. An equilibrium temperature of 2CuO and Cu_2O is about 1,025°C in air, meaning that the $\text{Cu}^+/\Sigma\text{Cu}$ ratio in the Bi-based glasses is affected by melting and quenching conditions. That is, many Cu ions in the melt of $\text{Bi}_2\text{Sr}_2\text{CaCu}_2\text{O}_x$ composition at 1,300°C would exist as Cu^+ ions. Zheng *et al.*²⁴⁾ prepared the $\text{Bi}_4\text{Sr}_3\text{Ca}_3\text{Cu}_4\text{O}_x$

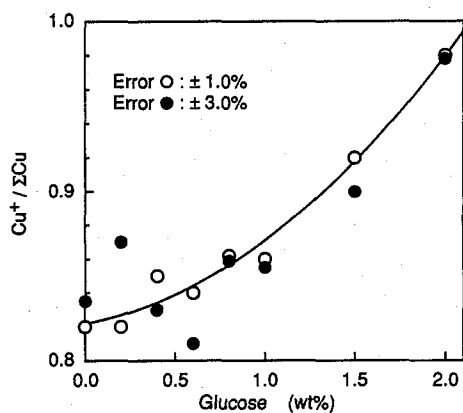


Fig. 3. Values of $\text{Cu}^+/\Sigma\text{Cu}$ in the $\text{Bi}_2\text{Sr}_2\text{CaCu}_2\text{O}_x$ glasses with added glucose of 0~2.0 wt%. \circ , the cerate titration method; \bullet , TG analyses.⁵⁾

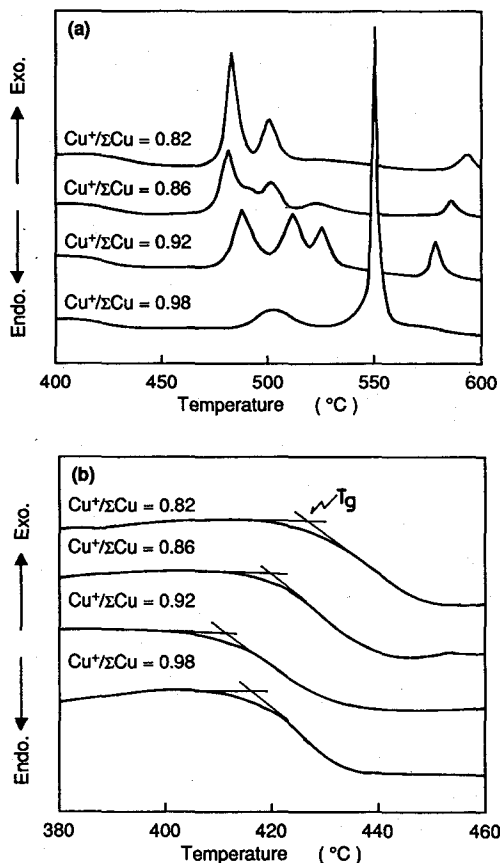


Fig. 4. DTA curves for the bulk $\text{Bi}_2\text{Sr}_2\text{CaCu}_2\text{O}_x$ glasses with different $\text{Cu}^+/\Sigma\text{Cu}$ ratios at temperature $>400^\circ\text{C}$ (a) and blown up near T_g (b).⁵⁾ Heating rate was 10 K/min.

glasses with different $\text{Cu}^+/\Sigma\text{Cu}$ ratios (0.66~0.85) by changing melting temperature. It is clear from Fig. 3 that the addition of glucose being a reducing agent accelerates the transformation of Cu^{2+} ions into Cu^+ ions in the melt of Bi-Sr-Ca-Cu-O system and is effective in controlling the copper valence in Bi-based glasses.

The DTA curves in air for the bulk $\text{Bi}_2\text{Sr}_2\text{CaCu}_2\text{O}_x$ glasses with the different $\text{Cu}^+/\Sigma\text{Cu}$ ratios are shown in Fig. 4(a) and (b). It is clear that the patterns are strongly dependent on the $\text{Cu}^+/\Sigma\text{Cu}$ ratio. It is noted that the onset temperature of the first crystallization peak shifts to higher temperature and the peak intensity decreases rapidly with increasing $\text{Cu}^+/\Sigma\text{Cu}$ ratio. The values of glass transition, T_g , crystallization onset, $T_{x_{on}}$, and peak, T_{x_p} , temperatures are shown in Fig. 5 as a function of $\text{Cu}^+/\Sigma\text{Cu}$ ratio. The value of T_g tends to decrease slightly with increasing $\text{Cu}^+/\Sigma\text{Cu}$ ratio. On the other hand, the values of $T_{x_{on}}$ and T_{x_p} for the glasses with up to $\text{Cu}^+/\Sigma\text{Cu}=0.85$ are almost the same, but those for the glass with $\text{Cu}^+/\Sigma\text{Cu}=0.98$ are high compared with other glasses. In the glass with $\text{Cu}^+/\Sigma\text{Cu}=0.98$, the difference between $T_{x_{on}}$ and T_g , $\Delta T=T_{x_{on}}-T_g$, was 70°C . It indicates that the thermal stability of $\text{Bi}_2\text{Sr}_2\text{CaCu}_2\text{O}_x$

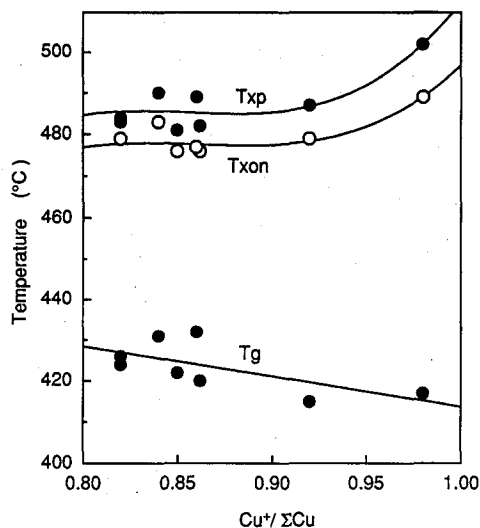


Fig. 5. Values of glass transition, T_g , crystallization onset, T_{xon} , and peak, T_{xp} , temperatures for the bulk $\text{Bi}_2\text{Sr}_2\text{CaCu}_2\text{O}_x$ glasses as a function of $\text{Cu}^+/\Sigma\text{Cu}$.⁵⁾

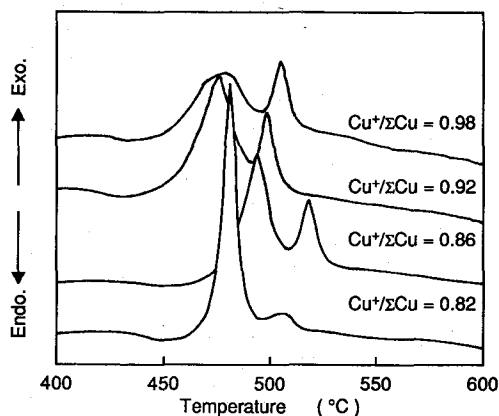


Fig. 6. DTA curves for the powdered $\text{Bi}_2\text{Sr}_2\text{CaCu}_2\text{O}_x$ glasses with different $\text{Cu}^+/\Sigma\text{Cu}$ ratios at temperature $>400^\circ\text{C}$.⁵⁾ Heating rate was 10 K/min.

glass is improved by increasing $\text{Cu}^+/\Sigma\text{Cu}$ ratio. Indeed, in the sample with $\text{Cu}^+/\Sigma\text{Cu}=0.98$, a perfect glass is obtained without any press (rapid quenching) but just pumping up (slow quenching) into silica glass tubes with 3 mm diameter.

Figure 6 shows the DTA curves for the powdered glasses with different $\text{Cu}^+/\Sigma\text{Cu}$ ratios. The value of T_g for the powdered glass is higher than that for the bulk glass with the same $\text{Cu}^+/\Sigma\text{Cu}$ ratio, and the value of T_{xon} is lower. The first exothermic peak due to the crystallization for powdered glasses is very broad. Figure 7 shows the TG curves for the bulk and powdered samples of the glass with $\text{Cu}^+/\Sigma\text{Cu}=0.98$, together with the DTA curves. In the powdered sample, an increase in the weight occurs rapidly at above 300°C and a gradual decrease is observed above 650°C . In the bulk sample, an increase in the weight is very small below 650°C and a rapid increase occurs at 700°C . The maximum increase is observed at around 850°C . The increase in the weight for the powdered sample occurs rapidly at temperature below T_x , indicating that in the powdered sample with large surface area the oxidation of Cu^+ to Cu^{2+} is accelerated. This oxidation would be a cause of the decrease in crystallization temperature for the powdered glasses. These results clearly indicate that the thermal stability of the Bi-based glasses in which Cu ions exist almost completely as Cu^+ ions is much higher than that of glasses in which a large amount of Cu^{2+} ions are included. Since the initial crystalline phase appearing during heating of the $\text{Bi}_2\text{Sr}_2\text{CaCu}_2\text{O}_x$ glass is the $\text{Bi}_2\text{Sr}_2\text{CuO}_x$ phase in which Cu ions exist almost completely as Cu^{2+} ions,^{5,24-29)} the presence of Cu^+ ions would decrease the rate of the crystallization of glasses.

Although the role of Cu^+ ion in the glass structure is not clear, it is expected that Cu^+ ions play an important role in the glass structure and that the structure of $\text{Bi}_2\text{Sr}_2\text{CaCu}_2\text{O}_x$ glass varies with copper valence state in glass. Nakagawa *et al.*³⁰⁾ investigated a local structure around Cu atoms in the $\text{Bi}_2\text{Sr}_2\text{CaCu}_2\text{O}_x$ glass by the EXAFS analysis and proposed that some fraction of Cu

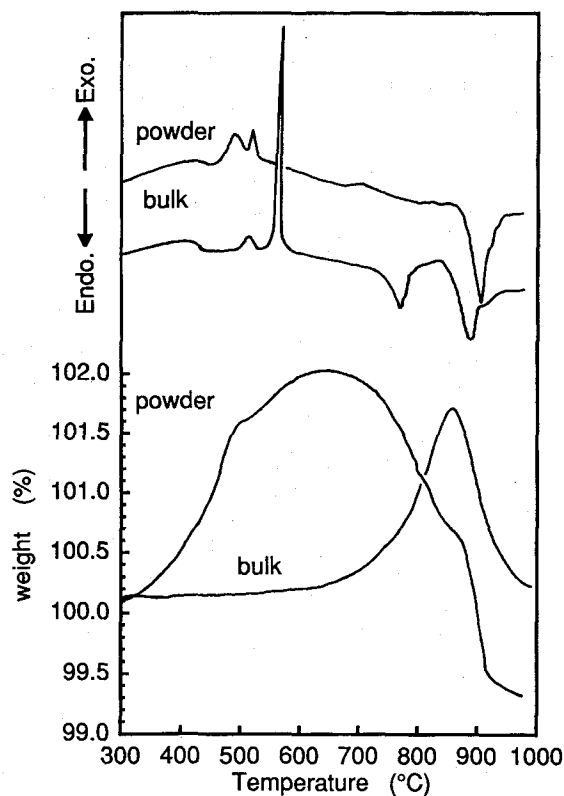


Fig. 7. TG and DTA curves for the bulk and powders of the $\text{Bi}_2\text{Sr}_2\text{CaCu}_2\text{O}_x$ glasses with $\text{Cu}^+/\Sigma\text{Cu}=0.98$.⁵⁾

ions exists as Cu^+ surrounded by two oxygen. Recently, Sato *et al.*⁷⁾ found that the viscosity and density of $\text{Bi}_2\text{Sr}_2\text{CaCu}_2\text{O}_x$ glass decrease rapidly with increasing $\text{Cu}^+/\Sigma\text{Cu}$ ratio and proposed that the structure of Bi-based glasses becomes loose with increasing $\text{Cu}^+/\Sigma\text{Cu}$ ratio.

It is worth to remind the effect of copper valence state on the structure and properties of copper aluminosilicate glasses. It is well recognized that Cu^+ ions play an important role in the unique properties of copper aluminosilicate glasses,³¹⁻³⁴⁾ i.e., low thermal expansions and low viscosities. Makishima *et al.*³²⁾ proposed that copper aluminosilicate glasses have low values of packing densities of atoms, and the low thermal expansion may correlate with an open structure. Kamiya *et al.*³⁴⁾ investigated a local structure around Cu atoms in copper aluminosilicate glasses by the EXAFS analysis and reported that the Cu^+ ion in copper aluminosilicate glasses is coordinated to two oxygens through covalent Cu^+-O bonds. They suggested that the Cu^+-O bond in copper aluminosilicate glasses is covalent as in Cu_2O and CuAlO_2 crystals, since Cu^+-O distance in the copper aluminosilicate glasses is 0.190 nm, which is relatively small compared to the sum of the Pauling's ionic radii of Cu^+ , 0.096 nm, and O^{2-} , 0.140 nm. Nakagawa *et al.*³⁰⁾ reported that the average Cu-O distance in the $\text{Bi}_2\text{Sr}_2\text{CaCu}_2\text{O}_x$ glass is 0.189 nm. These studies support the suggestion that the structure of Bi-based glass varies significantly with the $\text{Cu}^+/\Sigma\text{Cu}$ ratio and the Cu^+-O bond in the $\text{Bi}_2\text{Sr}_2\text{CaCu}_2\text{O}_x$ glass is also covalent. The increase in the covalency of Cu^+-O bonds would be a significant reason for the improvement of thermal stability

for the Bi-based glasses with high $\text{Cu}^+/\Sigma\text{Cu}$ ratios.

4. PHYSICAL PROPERTY OF $\text{Bi}_2\text{Sr}_2\text{CaCu}_2\text{O}_x$ GLASS

The effect of $\text{Cu}^+/\Sigma\text{Cu}$ ratio on the density of the $\text{Bi}_2\text{Sr}_2\text{CaCu}_2\text{O}_x$ glass is shown in Fig. 8 as a function of $\text{Cu}^+/\Sigma\text{Cu}$ ratio. The density decreases almost linearly with increasing Cu^+ content. The large decreases imply that the structure of glasses changes with the Cu^+ content. If one assumes that the structures of the glasses such as $\text{Bi}_2\text{Sr}_2\text{CaCu}^+_{1.6}\text{Cu}^{2+}_{0.4}\text{O}_{7.2}$ and $\text{Bi}_2\text{Sr}_2\text{CaCu}^+_{1.9}\text{Cu}^{2+}_{0.1}\text{O}_{7.05}$ are the same and the difference in the density arises only from oxygen content, the density change with the $\text{Cu}^+/\Sigma\text{Cu}$ ratio is expected as shown by a dotted line in Fig. 8. It is known that the oxygen coordination numbers of Cu ions in Cu_2O and CuO crystals are two and four, respectively and the densities of Cu_2O and CuO crystals are 6.04 and 6.31 g/cm^3 , respectively. If the oxygen coordination numbers of Cu ions in Bi-based glasses are similar to those in the crystals, i.e. two for Cu^+ ions and four or five for Cu^{2+} ions, a large decrease in the density would be expected, as is the case shown in Fig. 8.

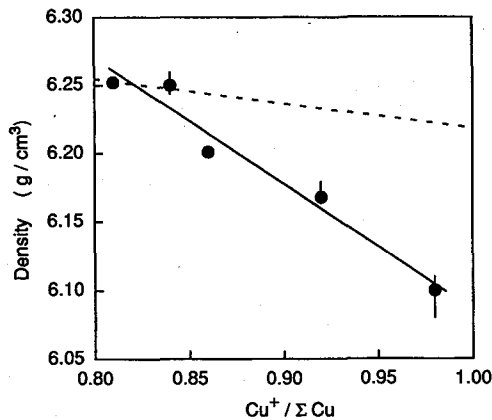


Fig. 8. Values of the density for the $\text{Bi}_2\text{Sr}_2\text{CaCu}_2\text{O}_x$ glasses with different $\text{Cu}^+/\Sigma\text{Cu}$ ratios.⁷⁾

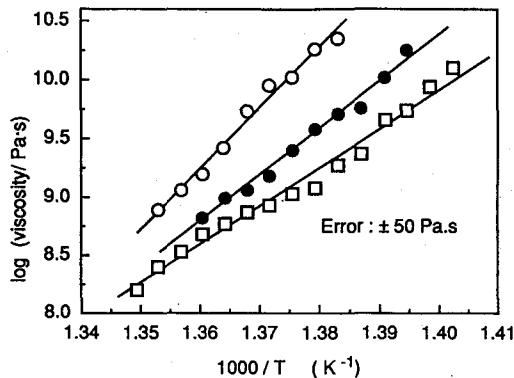


Fig. 9. Temperature dependence of viscosity for the $\text{Bi}_2\text{Sr}_2\text{CaCu}_2\text{O}_x$ glasses with different $\text{Cu}^+/\Sigma\text{Cu}$ ratios: \circ , $\text{Cu}^+/\Sigma\text{Cu}=0.82$; \bullet , $\text{Cu}^+/\Sigma\text{Cu}=0.88$; \square , $\text{Cu}^+/\Sigma\text{Cu}=0.98$.⁷⁾

The viscous flow behaviors were also reported.⁷⁾ The Arrhenius plots of the viscosity of the glasses with different $\text{Cu}^+/\Sigma\text{Cu}$ ratios are shown in Fig. 9. It is seen that the viscosity in the temperature range of 431 and 467°C obeys the Arrhenius law. The isoviscous temperatures of these glasses decrease with increasing Cu^+ content. The activation energies, E_a , for viscous flow estimated from the data in Figs. 9 are shown in Fig. 10 as a function of $\text{Cu}^+/\Sigma\text{Cu}$ ratio. The value of E_a decreases rapidly with increasing Cu^+ content from 987 to 637 kJ/mol. These values for the $\text{Bi}_2\text{Sr}_2\text{CaCu}_2\text{O}_x$ glasses are similar to the values of 800~980 kJ/mol for $\text{Bi}_x\text{SrCaCu}_2\text{O}_y$ glasses ($x=1.5$ and 2.7) reported by Tatsumisago *et al.*³⁵⁾ The results shown in Figs. 9 and 10 indicate that the viscosity of Bi-based glasses is very sensitive to the copper valence state. In other words, the decrease of E_a for the viscous flow indicates that the size of flow unit decreases with increasing Cu^+ content or the amount of free volume increases. It is clear that the dependence of the copper valence state on the viscosity shown in Figs. 9 and 10 is very similar to that on the density shown in Fig. 8, suggesting again that the structure of Bi-based glasses becomes loose with increasing Cu^+ content.

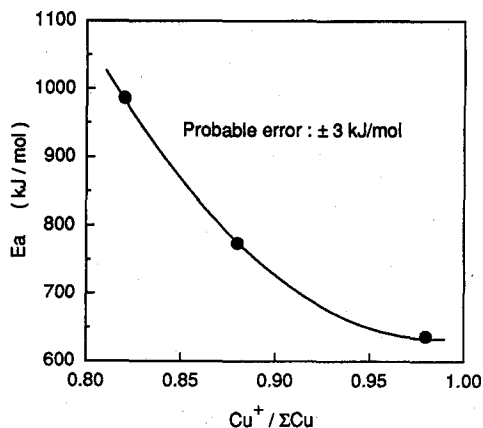


Fig. 10. Values of the activation energy, E_a , for viscous flow estimated from Arrhenius plot (Fig. 9) for the $\text{Bi}_2\text{Sr}_2\text{CaCu}_2\text{O}_x$ glasses with different $\text{Cu}^+/\Sigma\text{Cu}$ ratios.⁷⁾

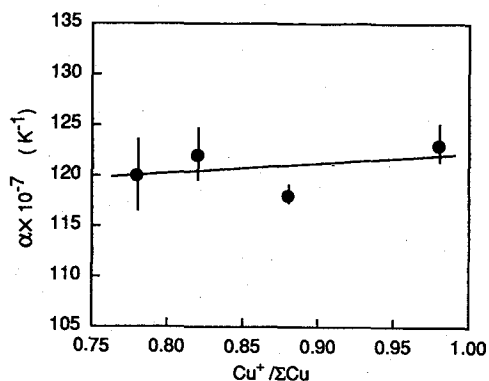


Fig. 11. Values of the thermal expansion coefficient, α , for the $\text{Bi}_2\text{Sr}_2\text{CaCu}_2\text{O}_x$ glasses with different $\text{Cu}^+/\Sigma\text{Cu}$ ratios.⁷⁾

The thermal expansion coefficients for the $\text{Bi}_2\text{Sr}_2\text{CaCu}_2\text{O}_x$ glasses are shown in Fig. 11 as a function of $\text{Cu}^+/\Sigma\text{Cu}$ ratio. The values obtained are about $120 \times 10^{-7} \text{ K}^{-1}$ and insensitive to the Cu^+ content. It is well known that the thermal expansion coefficient of ordinary oxide glasses containing copper ions such as $\text{Cu}_2\text{O} \cdot \text{Al}_2\text{O}_3 \cdot 4\text{SiO}_2$ depends strongly on the $\text{Cu}^+/\Sigma\text{Cu}$ ratio.³⁶⁾ For Bi-based glasses with low Cu^+ contents such as $\text{Cu}^+/\Sigma\text{Cu} \leq 0.5$, if possible, some change in the thermal expansion coefficient might be observed.

5. OXIDATION OF Cu^+ IONS IN $\text{Bi}_2\text{Sr}_2\text{CaCu}_2\text{O}_x$ GLASS

The preparation and investigation of the Bi-based glasses with high Cu^{2+} contents are very important. However, the Bi-based glasses with high Cu^{2+} contents can not be prepared by using a conventional melt-quenching method. Very recently, Sato *et al.*¹⁰⁾ succeeded in

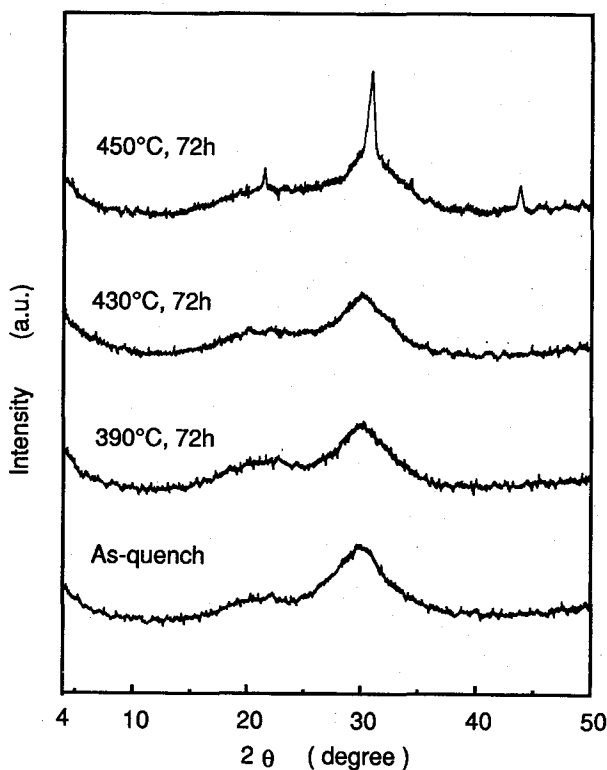


Fig. 12. XRD powder patterns at room temperature for the $\text{Bi}_2\text{Sr}_2\text{CaCu}_2\text{O}_x$ samples annealed at near the glass transition temperature (390, 430, 450°C) for 72 h in oxygen.¹⁰⁾

preparing the $\text{Bi}_2\text{Sr}_2\text{CaCu}_2\text{O}_x$ glass powders with low Cu^+ contents, i.e. $\text{Cu}^+/\Sigma\text{Cu}=0.01\sim 0.8$, by oxidizing of Cu^+ to Cu^{2+} through the annealing in oxygen at near the glass transition temperature without causing any crystallization. In their experiment, the bulk glass was first ground, and then the glass powders with diameters less than $37\ \mu\text{m}$ were oxidized.

Figure 12 shows X-ray powder diffraction patterns at room temperature for the samples annealed at 390, 430 and 450°C for 72 h in oxygen. In the as-quenched glass, a large halo is observed at around $2\theta=30^\circ$ and a small one is also observed at around $2\theta=20^\circ$. The value of the half width of the large halo is about 5.5° . In the powdered samples annealed at 390°C and 430°C, a large halo is also observed and any sharp diffraction peak can not be seen. The values of the half width of these large halos are almost the same as that of as-quenched glass. An annealing at 450°C leads to the appearance of the peaks due to the precipitation of a crystalline phase. This phase is assigned to the $\text{Bi}_2\text{Sr}_2\text{CuO}_y$ phase. These results indicate that the glassy state is kept in the powdered glasses annealed at 430°C for 72 h in oxygen but a crystallization occurs at annealing of about 450°C.

The values of the $\text{Cu}^+/\Sigma\text{Cu}$ ratio analyzed by a cerate titration for the powdered glasses annealed at 430°C are shown in Fig. 13 as a function of annealing time. A decrease in the $\text{Cu}^+/\Sigma\text{Cu}$ ratio occurs rapidly within a short annealing time below 4 h. This result indicates that the Cu^+ ions in the powdered glasses are easily oxidized through the annealing at 430°C

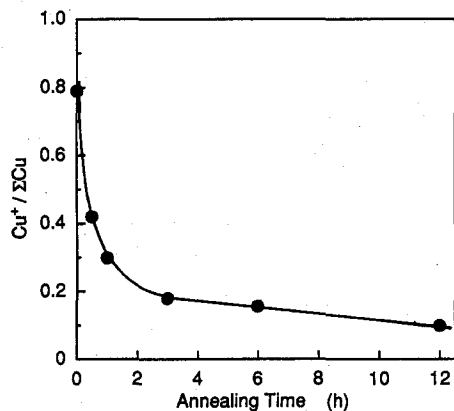


Fig. 13. Plots of $\text{Cu}^+/\Sigma\text{Cu}$ ratio against annealing time for the $\text{Bi}_2\text{Sr}_2\text{CaCu}_2\text{O}_x$ samples obtained by annealing at 430°C .¹⁰⁾

without causing any crystallization, i.e. with keeping the amorphous state.

The DTA curves in oxygen for the powdered glasses annealed at 430°C for various periods in oxygen are shown Fig. 14. The exothermic peaks due to the crystallization are observed in all glasses. In the as-quenched glass, two exothermic peaks are observed at around 460 and 500°C . In the annealed samples, the intensity of the exothermic peak at around 460°C decreases with increasing annealing time and such a peak is not observed in the glass annealed for 180 min. On the other hand, the intensity of the exothermic peak at around 500°C increases with increasing annealing time. Figure 15 shows the expanded DTA curves at near the glass transition for the

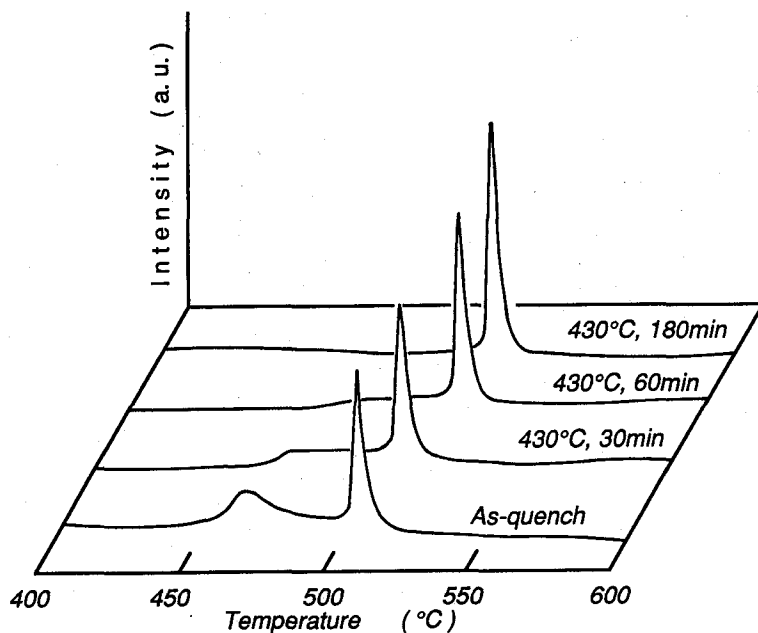


Fig. 14. DTA curves for the $\text{Bi}_2\text{Sr}_2\text{CaCu}_2\text{O}_x$ samples annealed at 430°C for various periods in oxygen.¹⁰⁾ Heating rate was 10 K/min.

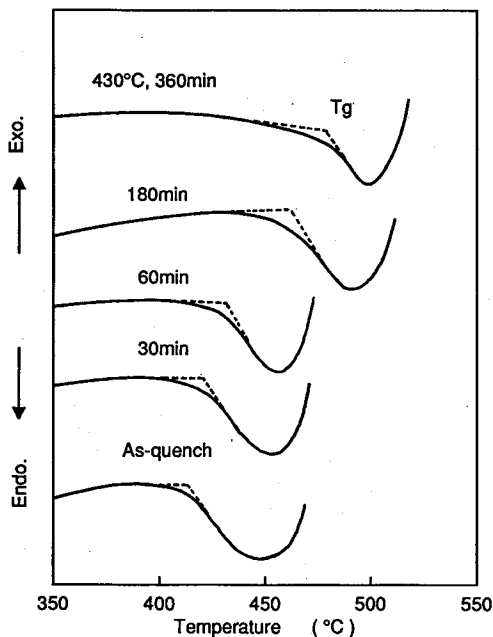


Fig. 15. Expanded DTA curves at near glass transition for the samples obtained by annealing at 430°C.⁹⁾

powdered glasses annealed at 430°C. The endothermic peak due to the glass transition is clearly observed in all glasses. This result also indicates that the glassy state is kept in the powdered glasses annealed at 430°C in oxygen. The values of Tg and Tx for the powdered glasses obtained by annealing in oxygen are given in Fig. 16 as a function of Cu⁺/ΣCu ratio. It is seen

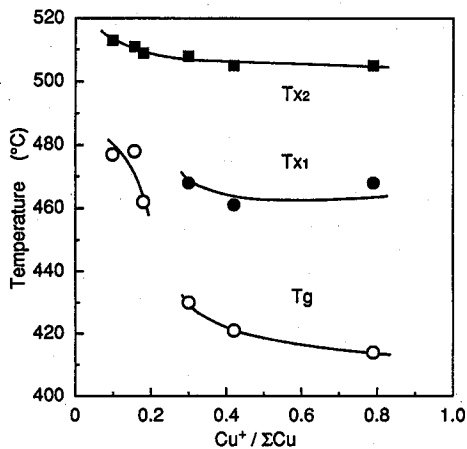


Fig. 16. Values of glass transition, Tg, crystallization onset, Tx, temperatures as a function of Cu⁺/ΣCu ratio for the Bi₂Sr₂CaCu₂O_x samples obtained by annealing at near the glass transition.¹⁰⁾

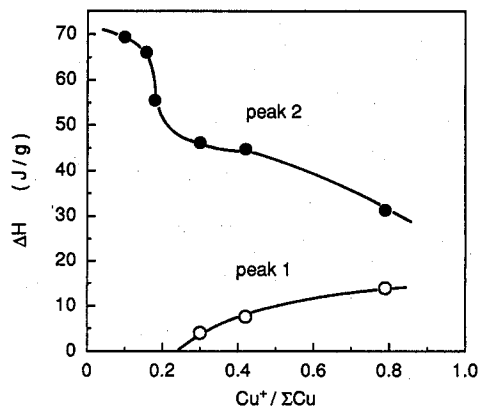


Fig. 17. Intensities of the exothermic peaks measured by DSC as a function of Cu⁺/ΣCu ratio for the Bi₂Sr₂CaCu₂O_x samples obtained by annealing at near the glass transition.¹⁰⁾

that the values of T_g or T_x for the glasses with $\text{Cu}^+/\Sigma\text{Cu} < 0.3$ are much higher than those for the glasses with $\text{Cu}^+/\Sigma\text{Cu} > 0.3$. The highest values of glass transition and crystallization temperatures are 474°C and 513°C , respectively. In Bi-based glasses, these are the highest values of all data reported so far.

The intensities of the exothermic peaks due to the crystallization for the $\text{Bi}_2\text{Sr}_2\text{CaCu}_2\text{O}_x$ powdered glasses, which were measured by a differential scanning calorimetry (DSC), are shown in Fig. 17 as a function of $\text{Cu}^+/\Sigma\text{Cu}$ ratio. The intensity of the first exothermic peak, DH, decreases gradually and that of the second crystallization peak increases with decreasing $\text{Cu}^+/\Sigma\text{Cu}$ ratio. Particularly, in the glasses with $\text{Cu}^+/\Sigma\text{Cu} < 0.2$, a rapid increase is observed. These results shown in Figs. 16 and 17 also indicate that the structure of the $\text{Bi}_2\text{Sr}_2\text{CaCu}_2\text{O}_x$ glass is largely affected by the $\text{Cu}^+/\Sigma\text{Cu}$ ratio and particularly changes drastically at around $\text{Cu}^+/\Sigma\text{Cu} = 0.2$.

6. MICROSTRUCTURE OF BI-BASED GLASSES

The microstructure of Bi-based glasses using transmission electron microscopy (TEM) has been reported by several researchers. Kim *et al.*⁸⁾ and Aruchamy⁹⁾ reported that the phase separation occurs in the $\text{Bi}_2\text{Sr}_2\text{CaCu}_2\text{O}_x$ glass and the $\text{Bi}_{1.68}\text{Pb}_{0.32}\text{Sr}_{1.75}\text{Ca}_2\text{Cu}_3\text{O}_x$ glass. However, the chemical compositions of those phases and the origin of the phase separation have not been clarified yet. Kasuga *et al.*³⁷⁾ reported that the addition of Al_2O_3 to a $\text{BiSrCaCu}_2\text{O}_x$ melt enhances a droplet-like phase separation.

The TEM micrograph of the as-quenched $\text{Bi}_2\text{Sr}_2\text{CaCu}_2\text{O}_x$ glass ($\text{Cu}^+/\Sigma\text{Cu} = 0.81$) is shown in Fig. 18. The electron diffraction pattern, which is inserted in the figure, is a typical amorphous ring. The microstructure shown in Fig. 18 has a characteristic of liquid-liquid phase separation, demonstrating that the as-quenched glass is phase separated. The feature size found

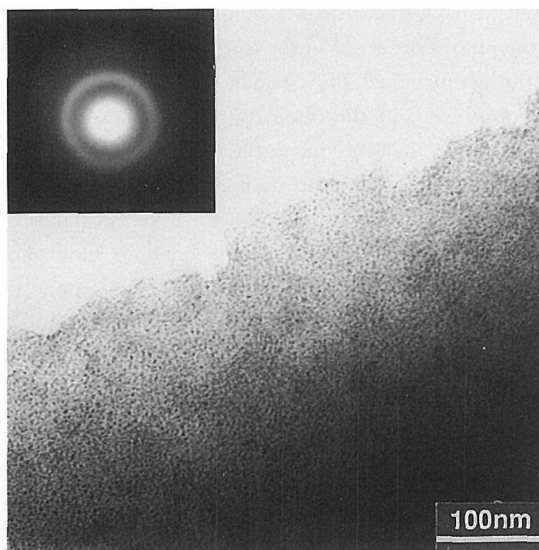


Fig. 18. TEM bright-field image from the as-quenched $\text{Bi}_2\text{Sr}_2\text{CaCu}_2\text{O}_x$ glass. Insert is an electron diffraction pattern.¹⁰⁾

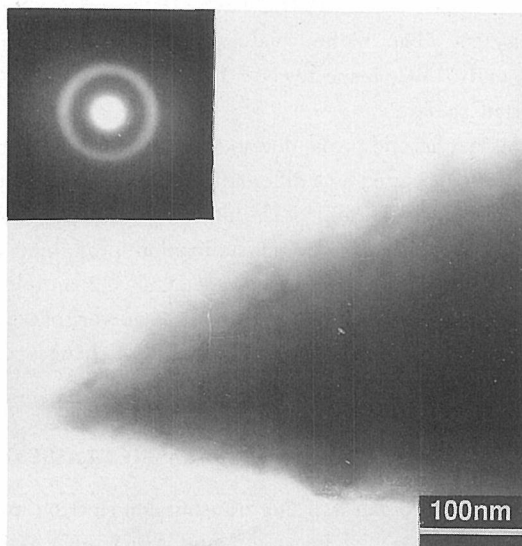


Fig. 19. TEM bright-field image from the $\text{Bi}_2\text{Sr}_2\text{CaCu}_2\text{O}_x$ specimen annealed at 430°C for 72 h in oxygen. Insert is an electron diffraction pattern.¹⁰⁾

in this sample is in the range of 4~10 nm. Similar microstructures were observed for some other Bi-based glasses.^{8,9)} Figure 19 shows the TEM micrograph of the $\text{Bi}_2\text{Sr}_2\text{CaCu}_2\text{O}_x$ glass ($\text{Cu}^+/\Sigma\text{Cu}=0.01$) annealed at 430°C for 72 h in oxygen. Any fine structure composed of clear different contrasts is not seen. This result suggests that the phase separation in the as-quenched glass disappears due to the annealing in oxygen. In other words, the phase separation behaviors of Bi-based glasses depend largely on the copper valence state. It is considered that the presence of Cu^+ ion in the $\text{Bi}_2\text{Sr}_2\text{CaCu}_2\text{O}_x$ glass is a key factor for the phase separation. That is, it is considered that one of the phases observed in the as-quenched glass contains most of Cu^+ ions. In the DTA curve of the as-quenched $\text{Bi}_2\text{Sr}_2\text{CaCu}_2\text{O}_x$ glass powders shown in Fig. 14, two exothermic peaks were observed and the intensity of lower exothermic peak decreased with decreasing $\text{Cu}^+/\Sigma\text{Cu}$ ratio. On the other hand, the intensity of the second peak increased with decreasing $\text{Cu}^+/\Sigma\text{Cu}$ ratio. These crystallization behaviors might be closely related to the phase separation behaviors. That is, the glasses with a phase separation have two crystallization peaks and the glasses with no phase separation have only one crystallization peak.

As shown in Fig. 16, a rapid increase in T_g was observed at around $\text{Cu}^+/\Sigma\text{Cu}=0.3$. It is known that some glasses in which a phase separation occurs have two glass transition temperatures.³⁸⁾ However, two glass transition temperatures are not observed in the $\text{Bi}_2\text{Sr}_2\text{CaCu}_2\text{O}_x$ glass, as shown in Fig. 15. In the glasses with $\text{Cu}^+/\Sigma\text{Cu}\geq 0.3$, the glass transition and lower crystallization temperatures are observed at about 420°C and 460°C , respectively. On the other hand, the glasses with $\text{Cu}^+/\Sigma\text{Cu}=0.01$, in which a phase separation is not observed, exhibited a glass transition at about 470°C . From these results, it would be expected that although the as-quenched glass separates into two glass phases having T_g of about 420°C and 470°C , an endothermic peak due to the higher glass transition is overlapped by the lower crystallization peak and would not be observed in a DTA curve.

ACKNOWLEDGEMENTS

The authors gratefully acknowledge the financial support of Mitsubishi CVable Ltd. in this work. The authors also thank Mr. T. Ohki, Mr. C. Hirose and Mr. Y. Kuken for the preparation of glasses.

REFERENCES

- (1) T. Komatsu, K. Imai, R. Sato, K. Matusita and T. Yamashita, *Jpn. J. Appl. Phys.*, **27**, L533-535 (1988).
- (2) T. Komatsu, R. Sato, K. Imai, K. Matusita and T. Yamashita, *Jpn. J. Appl. Phys.*, **27**, L550-552 (1988).
- (3) D.G. Hinks, L. Soderholm, D.W. Capone, II, B. Dabrowski, A.W. Mitchell and D. Shi, *Appl. Phys. Lett.*, **53**, 423425 (1988).
- (4) T. Minami, Y. Akamatsu, M. Tatsumisago, N. Tohge and Y. Kowada, *Jpn. J. Appl. Phys.*, **27**, L777-778 (1988).
- (5) R. Sato, T. Komatsu, Y. Kuken, K. Matusita, K. Sawada and M. Hiraoka, *J. Non-Cryst. Solids*, **152**, 150-156 (1993).
- (6) T. Komatsu, R. Sato, Y. Kuken and K. Matusita, *J. Am. Ceram. Soc.*, **76**, 2795-2800 (1993).
- (7) R. Sato, T. Komatsu and K. Matusita, *J. Non-Cryst. Solids*, **160**, 180-182 (1993).
- (8) S.J. Kim, D.P. Birnie III, A. Aruchamy, D.R. Uhlmann, O.H. El-Bayoumi and M.J. Suscavage, *Physica C*, **191**, 316-320 (1992).
- (9) A. Aruchamy, S.J. Kim, D.P. Birnie III and D.R. Uhlmann, *J. Non-Cryst. Solids*, **160**, 60-67 (1993).
- (10) R. Sato, T. Komatsu and K. Matusita, *J. Non-Cryst. Solids* in press.
- (11) T. Komatsu, T. Ohki, T. Matusita and T. Yamashita, *J. Ceram. Soc. Japan*, **97**, 251-255 (1989).
- (12) F. Miyaji, T. Yoko and S. Sakka, *J. Non-Cryst. Solids*, **126**, 170-172 (1990).
- (13) N. Tohge, S. Tsuboi, Y. Akamatsu, M. Tatsumisago and T. Minami, *J. Ceram. Soc. Japan*, **97**, 335-338 (1989).
- (14) H. Zheng, R. Xu and J.D. Mackenzie, *J. Matr. Res.*, **4**, 911 (1989).
- (15) Y. Dimitriev, B. Samuneva, Y. Ivanova, E. Gattef, V. Mihailova and A. Staneva, *Supercond. Sci. Technol.*, **3**, 606 (1990).
- (16) F. Gan and G. Li, *J. Non-Cryst. Solids*, **130**, 67 (1990).
- (17) H. Sato, W. Zhu and T. Ishiguro, *J. Solid State Chem.*, **75**, 207 (1988).
- (18) M. Yoshimura, T.H. Sung, Z. Nakagawa and T. Nakamura, *Jpn. J. Appl. Phys.*, **27**, L1877-1879 (1988).
- (19) H. Zheng and J.D. Mackenzie, *Phys. Rev. B*, **38**, 7166 (1988).
- (20) K.B.R. Varma, K.J. Rao and C.N.R. Rao, *Appl. Phys. Lett.*, **54**, 69 (1989).
- (21) B.K. Chaudhuri, K. Som and S.P.S. Gupta, *J. Mater. Sci. Lett.*, **8**, 520 (1989).
- (22) Y. Oka, N. Yamamoto, H. Kitaguchi, K. Oda and J. Takada, *Jpn. J. Appl. Phys.*, **28**, L213-216 (1989).
- (23) T. Komatsu, T. Ohki, C. Hirose and K. Matusita, *J. Non-Cryst. Solids*, **113**, 274-281 (1989).
- (24) H. Zheng, M.W. Colby and J.D. Mackenzie, *J. Non-Cryst. Solids*, **127**, 143-150 (1991).
- (25) T. Komatsu and K. Matusita, *Thermochim. Acta*, **174**, 131-151 (1991).
- (26) M. Tatsumisago, C.A. Angell, Y. Akamatsu, S. Tsuboi, N. Tohge and T. Minami, *Appl. Phys. Lett.*, **55**, 600-602 (1989).
- (27) M.R. De Guire, N.P. Bansal and C.J. Kim, *J. Am. Ceram. Soc.*, **73**, 1165-1171 (1990).
- (28) N. Tohge, S. Tsuboi, M. Tatsumisago and T. Minami, *Jpn. J. Appl. Phys.*, **28**, L1742-1745 (1989).
- (29) T.G. Holesinger, D.J. Miller and L.S. Chumdley, *J. Mater. Res.*, **7**, 1658-1671 (1992).
- (30) Z. Nakagawa, H. Morikawa, T.H. Sung, M. Yashimura, M. Maruno and Y. Udagawa, *J. Chem. Soc. Jpn.*, **12**, 2085-2087 (1989).
- (31) T. Takamori, A. Reisman and M. Rerkenblit, *J. Am. Ceram. Soc.*, **59**, 312 (1976).
- (32) A. Makishima, T. Utsugi and T. Sakaino, *J. Am. Ceram. Soc.*, **62**, 224 (1979).
- (33) K. Matusita and J.D. Mackenzie, *J. Non-Cryst. Solids*, **30**, 285 (1979).
- (34) K. Kamiya, K. Okasaka, M. Wada and H. Nasu, *Am. Ceram. Soc.*, **75**, 477-478 (1992).
- (35) M. Tatsumisago, C.A. Angell, S. Tsuboi, Y. Akamatsu, N. Tohge and T. Minami, *Appl. Phys. Lett.*, **54**, 2268-2270 (1989).
- (36) T. Yoko, K. Kamiya and S. Sakka, *J. Non-Cryst. Solids*, **71**, 245-251 (1985).
- (37) T. Kasuga and Y. Abe, *J. Am. Ceram. Soc.*, **76**, 1885-1887 (1993).
- (38) J.E. Shelby, *J. Non-Cryst. Solids*, **49**, 287-298 (1982).